International Gas Union Research Conference 2011

AN EXPERIMENTAL AND NUMERICAL INVESTIGATION OF PREMIXED FLAME PROPAGATION IN CONFINED/SEMI-CONFINED EXPLOSION CHAMBER

Main Author

Hibiki Ryuzaki

Technology Research Institute, Tokyo Gas

1-7-7, Suehiro-cho, Tsurumi-ku, Yokohama City, Kanagawa Pref. JAPAN

Co-author

R. Tominaga

Technology Research Institute, Tokyo Gas

1-7-7, Suehiro-cho, Tsurumi-ku, Yokohama City, Kanagawa Pref. JAPAN

1. ABSTRACT

This paper reports the latest achievements on the gas explosion experiments in a confined/semi-confined explosion chamber using methane/air mixtures, and calculations reproduced based thereon by CFD. A medium-sized chamber with a volume of 216 L was used to perform experiments. There have been only a few examples in which the overpressure history of a gas explosion has been measured using a constant-volume chamber of this scale. In order to confirm the scale dependence of the gas explosion phenomenon, a comparison of the results with those obtained through small-scale experimentation using a chamber with a volume of 8 L was also performed in this study. The difference between the two overpressure histories was found. The cause of this difference is the difference in flame development characteristics in chambers of different volumes, revealing the scale dependence of the explosion phenomenon. In addition, utilization of CFD is also important in the analysis of explosion-related incidents. Hence, computational grids with the same shapes but different scales are created to confirm the reproducibility of pressure history.

TABLE OF CONTENTS

2. Introduction

Because it can be supplied stably and offers ecological benefits, natural gas is expected to serve as a key component in Japan's energy strategy, and it will play an increasingly important role in the creation of a low carbon society. In order to use natural gas safely, it is imperative to have a precise understanding of its characteristics. For this reason, Tokyo Gas performs research and development to further enhance safety, constantly introducing the latest scientific knowledge about gas leakage, diffusion, and explosion. By putting such knowledge to practical use, safety design requirements and preventive measures against accidents in gas facilities can be formulated.

This paper reports the latest achievements from explosion experiments in confined/semi-confined explosion chambers using methane/air mixtures and related reproduction calculations conducted in our laboratory. When an explosion accident occurs in a confined or semi-confined space such as a living area, the degree of damage caused by the explosion mainly depends on the overpressure history (maximum pressure and rise velocity). Therefore, it is extremely useful for safety design to have as clear and as accurate an understanding of overpressure history as is possible. Nevertheless, it is known that there are numerous forms of gas explosions, and overpressure history differs based on type of flammable gas, dimensions of the surrounding space, and the like[1].

Based on these characteristics, the overpressure history of gas explosions has been studied using a confined/semi-confined small-scale chamber with a volume of roughly a few liters[2, 3]. In addition, full-scale gas explosion experiments, though few in number, have been performed[4, 5]. However, in this kind of experiment, sometimes a slight difference in initial experimental conditions might cause differences of several orders of magnitude in maximum pressure. In addition, it has been reported that the number of pressure peaks occurring ranges from a single peak to about four peaks[6], and the times at which these peaks occur varies greatly depending on experimental conditions. A recent study pointed out the necessity of considering the effect of external explosion when estimating pressure peaks inside a chamber[4]. Moreover, the strong scale dependence of the explosion phenomenon presents difficulties in terms of pressure peak prediction. For all of the above reasons, it is excessively difficult to accurately reproduce the overpressure history obtained in an actual-scale experiment in a small constant-volume chamber with an inner volume of a few liters, making it difficult to say that any such attempt has been successful until now.

Therefore, from the viewpoint of establishing safety design techniques for gas facilities, it is desirable to perform experiments using sizes that correspond as closely as possible to actual scales. Generally, however, it is unrealistic to expect access to experimental equipment having a scale of a few thousand liters or more.

Consequently, in this study, a medium-sized chamber (Type A) with a volume of 216 L was used to

perform experiments. The volume of this chamber is ten times or more the volume of a small-scale chamber used in the preceding studies described above. There are only a few examples in which the pressure history of an explosion has been measured using a chamber of this scale[7, 8], and thus the experiments exemplified herein will be of value in connecting results from small-scale chambers with those from full-scale explosion experiments. In addition, in order to confirm the scale dependence of the explosion phenomenon directly, comparison with the results obtained through similar small-scale experiments (inner volume of 8 L; Type B) conducted in the past was also performed[9].

3. Experimental Setup and Conditions

Fig. 1 shows the chamber used in the experiments. This chamber is made of rolled steel (SS400), with inner dimensions of 600 x 600 x 600 mm^3 and a volume of 216 L. For the observation of flames, only the front plate is made of acrylic plastic, while the entire wall of the chamber is painted in black to make it easier to observe flames. The removable side panels of the chamber also make it possible to conduct venting tests.

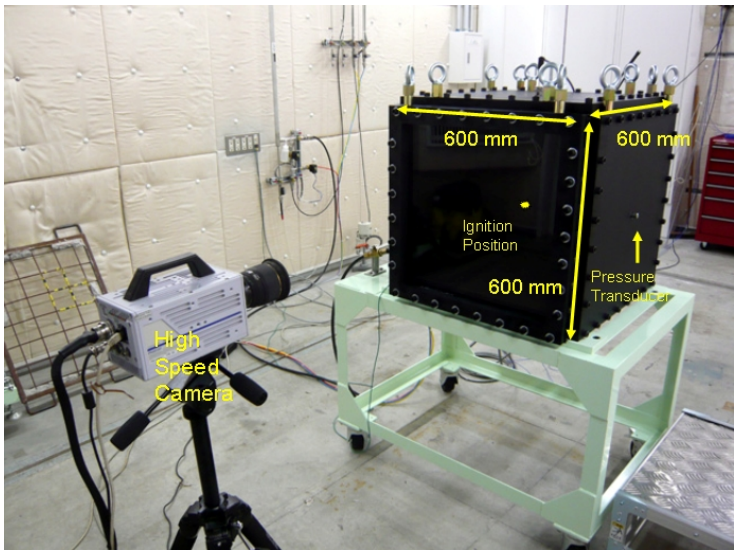

Fig. 1 Medium-sized explosion chamber used in experiments

A high speed camera (FASTCAM SA3, Photron) is used to observe the flames. The frame rate is 2,000 FPS, and a spark plug is used for ignition. The ignition position is at the center of the chamber. It is possible to ignite mixtures at any position inside the chamber by changing the length and positioning of the electrodes. A pressure sensor (M102B06, PCB) is mounted on the center of a side panel of the chamber. In the present study, measurement data was acquired using a data logger (GR-7500, Keyence). The sampling rate was set to 10^4 Hz. The fuel (methane and air), which were adjusted to a prescribed flow rate by flow meters, passed into a mixer in which they were mixed, following which they entered the chamber. In addition, the chamber contains a stirring fan, and after the mixed gas had traveled over a volume that was at least five times the inner volume of the chamber while the stirring

fan was being operated. Then the stirring fan was stopped and intake/exhaust valve was shut off at the same time. After being left to stand for 10 minutes, the mixture was ignited.

4. Results

4.1 Characteristics of Overpressure Histories in Confined Chambers

First, overpressure history and flame propagation were observed for premixed methane and air mixtures under various excess air ratios. Fig. 2 shows flame propagation behavior (excess air ratio = 1.00) inside the confined chamber photographed by a high-speed camera. It was observed that the flame spread around the ignition position in a spherical shape while increasing in brightness. Since the chamber is cube-shaped, as the flame grows, it touches the inside wall of the chamber and its shape becomes distorted. It was also observed that with the development of a flame, the wrinkle structure becomes fine and irregularities also grow.

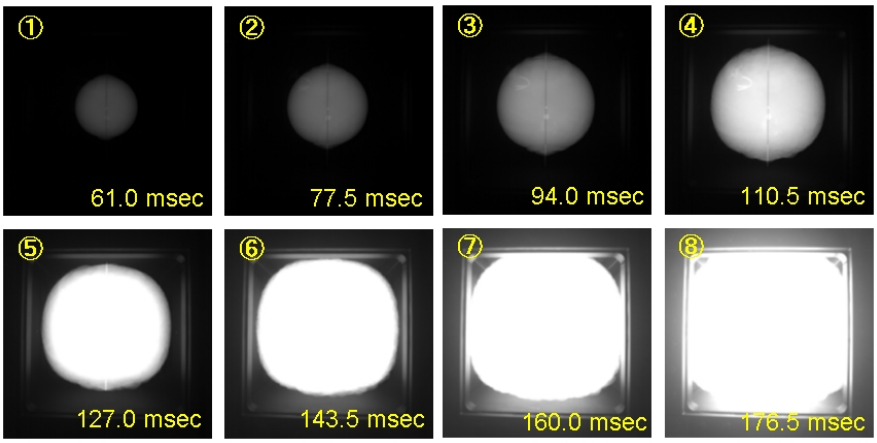

Fig. 2 Flame propagation in Type A chamber (excess air ratio = 1.00)

This tendency of the flame to experience destabilization was more conspicuous, such as when the excess air ratio deviated from 1.00 (Fig. 3). In addition, because the burning speed drops further as the excess air ratio deviates from 1.00, it was observed that the flame ball tends to be distorted in an upward direction due to the influence of buoyancy (Fig. 4).

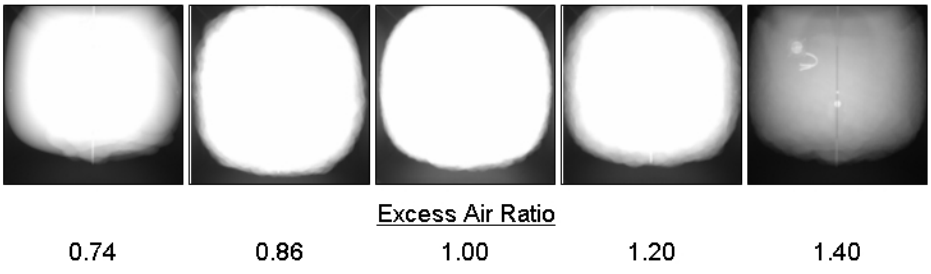

Fig. 3 Destabilizing tendency of propagating flame inside Type A chamber

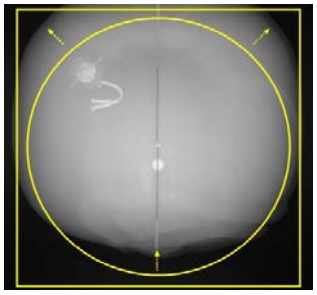

Fig. 4 Upward distortion of propagating flame affected by buoyancy

Figure 5 shows the results of the comparison of both overpressure histories. Because the length of a side of the Type A chamber is three times longer than that of a side of the Type B chamber, the time scale of the pressure history obtained with the experiment using the Type B chamber is derived by enlarging the time scale for the Type A chamber three times.

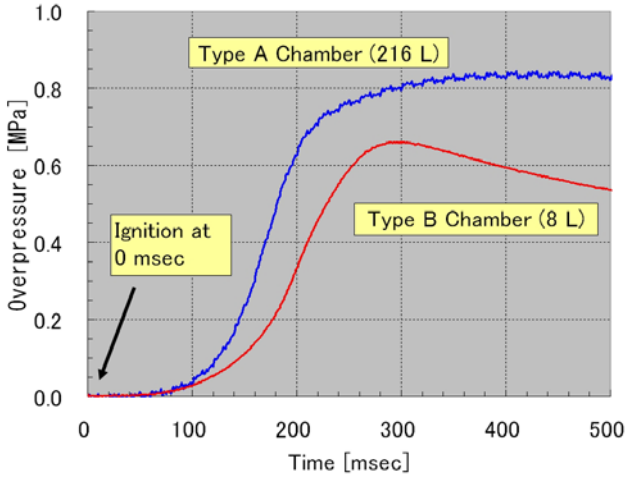

Fig. 5 Comparison of overpressure histories in chambers with different volumes (confined)

As is obvious from the comparison of two overpressure histories, a difference between the two pressure histories was found. This was a result of the difference of the flame development characteristics in chambers of different volumes, revealing the scale dependence of the explosion phenomenon.

Generally, because a propagating flame develops instability with the progress of time while also increasing propagation speed, the greater the size of the chamber, the greater the the propagation speed. On the other hand, as the flame grows and comes into contact with the inner wall of the chamber, because reaction heat is lost at that point, it becomes difficult for the flame to grow. This effect becomes smaller as the size of the chamber increases. This is because the total area of the chamber inner wall (which absorbs the reaction heat) does not increase to as great an extent as the flame volume (which generates the reaction heat) when the chamber size becomes larger. From these two

effects, as the chamber size becomes larger, the acceleration effect of flame becomes prominent, and there is an increase in the speed at which the pressure rises. Moreover, since the rate of heat loss by the inner wall decreases relatively, the maximum pressure also increases. The results shown in Fig. 5 provide support for these concepts.

In an attempt to conform the overpressure histories of explosions with two different scales, it is understood that not only conversion of time scale but also consideration of the precise mechanism of the explosion phenomenon are indispensable.

4.2 Characteristics of Overpressure Histories in Semi-confined Chambers

Next, a vent area was provided in the Type A chamber and similar experiments were conducted. The vent area used in this experiment is an aluminium plate 310 mm in diameter and 0.2 mm in thickness. Normally, in an explosion experiment inside a chamber having a vent area, vent coefficient (K) is used when judging scale dependence. When the volume of the chamber is V and the area of the vent area is A, the relationship $K = V^{2/3}/A$ pertains. In this experiment, K = 4.77. Fig. 6 shows the result of two successive tests conducted under almost the same conditions (the methane concentrations were slightly different). It must be noted that the unit of pressure is [kPa] (rather than [MPa], as in Fig. 5). Two pressure peaks were observed in each test. Confirmation via video images from a high-speed camera revealed that the 1st pressure peak appeared by the rupture of the vent area. However, the pressure did not rapidly decrease just after the rupture of the vent area -- instead, it continued to increase even after a certain period of time had passed following the rupture. As a result of analysis, in the two experiments described in Fig. 6, both rupture pressures were found to be 40.4 kPa.

The reproducibility of the 2nd pressure peak was not excellent. Although both experiments showed nearly the same pressure history up to the attenuation of the 1st pressure peaks, the 2nd pressure peaks gave results that differed by 30 kPa or greater. Confirmation of visual details using the high-speed camera revealed that the pressure peaks were generated by combustion of unburned gas remaining inside the chamber after burned gas is expelled due to the rupture of the vent area. Therefore, the large difference between the 2nd pressure peaks in the two successive experiments may have been caused by the fact that the amounts of unburned gas remaining inside the chamber were quite different in both cases. The blast flow of the burned gas caused by the rupture of the vent area is strong and turbulent, and it spreads outward, also engulfing the unburned gas. For this reason, it is considered that a slight difference in flow might result in a large change in the amount of unburned gas inside the chamber. In addition, in contrast to the 1st pressure peak, the 2nd pressure peak includes numerous vibration components. This is estimated to be the effect of acoustic vibration of the chamber[6]. It is a resonance phenomenon involving the constant-volume chamber and the propagating flame. In both of the experiments described in Fig. 6, the frequency of vibration was about 650 Hz.

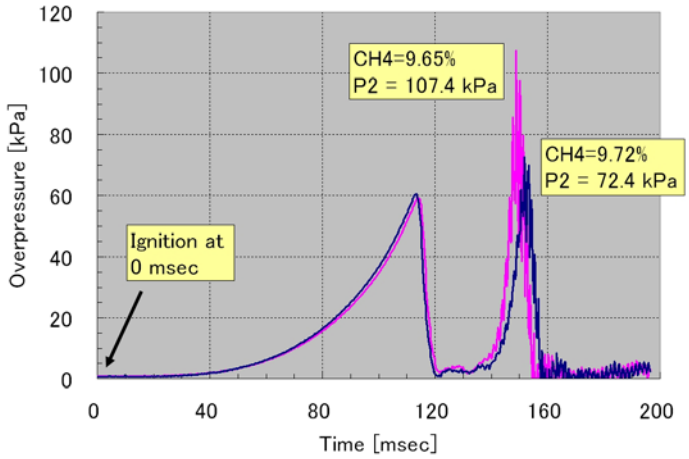

Fig. 6 Large fluctuation of the 2nd pressure peak

Fig. 7 is an image from the high-speed camera used in the experiment for CH_4 = 9.72% depicted in Fig. 6. Although the wrinkle structure on the flame surface disappears for a moment at the same time as the rupture of the vent area, thereafter, the formation of a conspicuous surface wrinkle can be recognized at the back end of the flame. It is considered that this represents an observation of “Rayleigh-Taylor instability”[10].

To confirm the effect of an external explosion, a flame jet blasted outside of the chamber is observed using a high-speed camera (Fig. 8). It was confirmed that the unburned gas that had been blasted from the chamber burned slightly immediately following the rupture of the vent area, but the formation of a large flame ball outside the chamber and the flow of burned gas back inside the chamber was not observed.

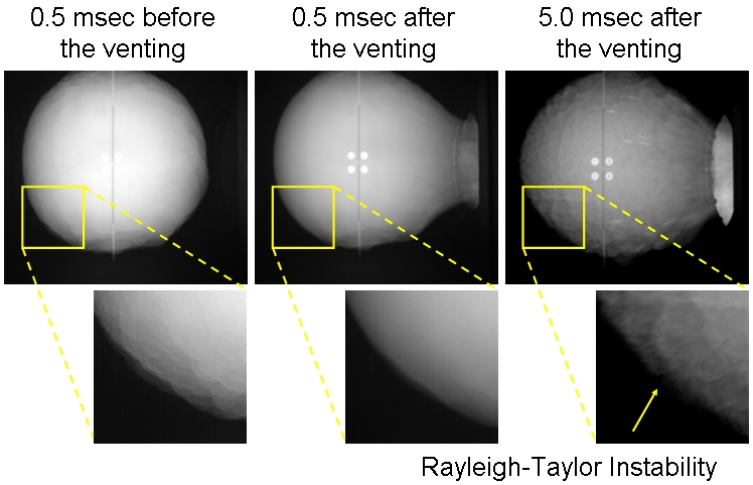

Fig. 7 Observation of Rayleigh-Taylor Instability at back end of flame

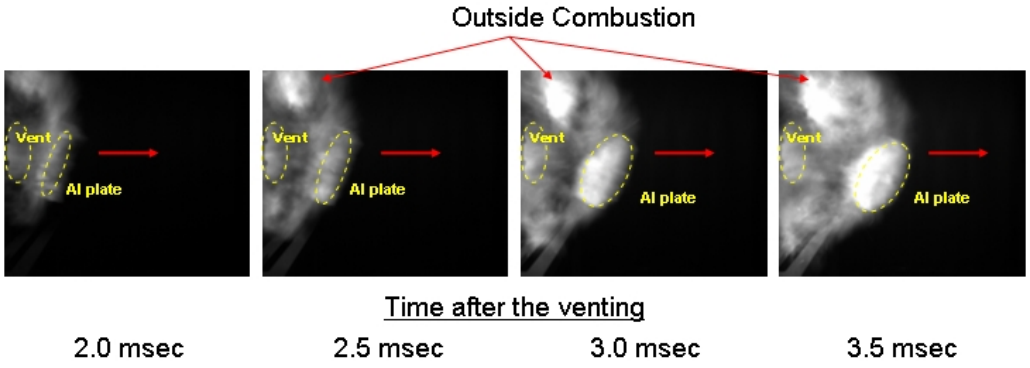

Fig. 8 Observation of jet flame after venting

For comparison, Fig. 9 shows experimental results for CH_4 = 9.72% depicted in Fig. 6 and similar experimental results (excess air ratio = 1.00; K = 4.77) for the Type B chamber. For the same reason as described above in relation to Fig. 5, the time scale was extended threefold for the results for the Type B chamber, taking the difference in chamber size into consideration. Attention must be paid that the vent area of each chamber was made of different material. As mentioned above, the vent area of the type A chamber was made of an aluminium plate while the vent area of the type B chamber was made of a translucent thin paper. Therefore it is highly difficult to extract the effect only part of the scale change from this result. In Fig. 9, however, scale dependence appears in a manner similar to the results of Fig. 5 and the rise velocity differs up to the 1st pressure peak. This is because the first pressure rise starts to increase well before the venting.

The most prominent difference is that the 2nd pressure peak does not exist in the results for the Type B chamber. Understanding the cause of this difference accurately is difficult at the present moment. However, when observing the overpressure histories of Fig. 9 in detail, for the experiment conducted in the Type B chamber, it was found that a negative pressure occurred after the rupture of the vent area, whereas the same could not be confirmed from the experimental results for the Type A chamber. Based on the foregoing, the mechanism by which the 2nd pressure peak is generated is thought to be as follows. First, it is considered that the negative pressure occurs because the vent area of the Type B chamber is made of translucent thin paper, which has a light mass; a flame jet is immediately blown out after the venting. Therefore, the amount of the unburned gas expelled from the chamber as if engulfed by this flame jet is relatively large, leaving not so much unburned gas inside the chamber to generate the 2nd pressure peak. On the other hand, the vent area of the Type A chamber is an aluminium plate that is much heavier than the translucent thin paper. Therefore, because it acts as a kind of resistance against the blast of the flame jet after the venting, the amount of the unburned gas expelled from the chamber as if engulfed by this flame jet is relatively small, leaving a sufficient amount of unburned gas inside the chamber to generate the 2nd pressure peak.

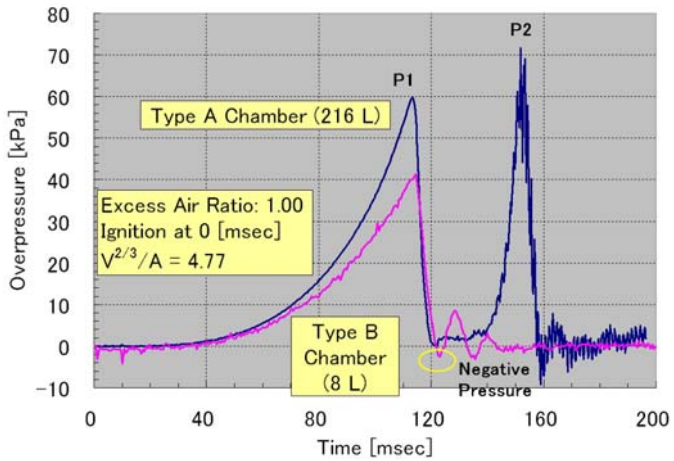

Fig. 9 Comparison of overpressure histories in chambers of different volumes (semi-confined)

Based on the above consideration, it is suggested that the cause of the 2nd pressure peak in this experiment might be understood not only as a problem of experimental scale but also in terms of differences in the mass of the vent area.

4.3 Numerical Calculation

In addition, in accident analysis, for which prompt responses are required, it is also effective to utilize CFD (Computational Fluid Dynamics). Therefore, computational grids having the same in form but different scales are created to confirm the reproducibility of overpressure history. FLACS is widely known as software used for analyzing the explosion phenomenon; however, because this software assumes a real-scale explosion incident, the scale differs vastly from the scales of the experiments of this study. Therefore, FIRE (ver. 2010, AVL) was used in this study. It is a multi-purpose thermo-fluid dynamics software that has been responsible for numerous actual achievements in the combustion analysis of internal combustion engines, and it includes a wide variety of combustion models and turbulence models. In addition, the difference from the assumed scale is not as great as that in the case of FLACS. Table 1 summarizes details on the calculation grids of the Type A chamber (confined) used in this study. Table 2 presents details on parameter settings.

Table 1 Details on calculation grids

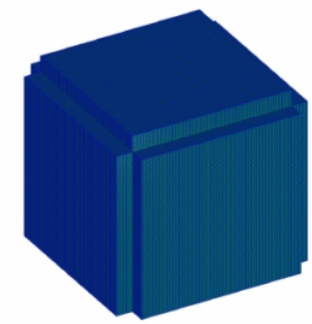

Global Mesh Size	: 5 mm
Total Mesh Number	: 1.7 million
Initial Pressure	: 1 atm
Initial Temperature	: 298 K
Equivalence Ratio	: 1.00
Closed System (No Inlet, No Outlet)	

Table 2 Details on parameter settings

Standard Settings	**Combustion**
Time step: 0.001 for the whole simulation	Model: ECFM
Discretization: Mirror and Least Sq. fit	Standard ignition model
Turbulence Model: k-zeta-f	Initial flame surface density: 20
Wall Treatment: Hybrid Wall Treatment	Stretch Factor: 2.8
Differencing Schemes for Momentum and Continuity: MINMOD Relaxed 1	Flame Kernel size: 0.005 m
	Ignition Duration: 0.005 s

Overpressure history is calculated using the above conditions. Fig. 10 shows the results. It can be confirmed that experimental results match with the calculation results with a high degree of precision. Fig. 11 illustrates the behavior of flame propagation. It has been possible to reproduce phenomenon of the flame glowing in a spherical shape as in the experimental results, and is distorted by the effect of the wall surface of the chamber. On the other hand, Fig. 12 shows the results of calculating overpressure history under the same conditions as those of Table 2 using the calculation grids of the Type B chamber (confined). For reasons similar to those described above, the time scale of the calculation results for the Type B chamber was extended threefold. Outcomes for the Type A chamber agreed with the experimental results with a high degree of precision, but outcomes for the Type B chamber differed therefrom to a great extent.

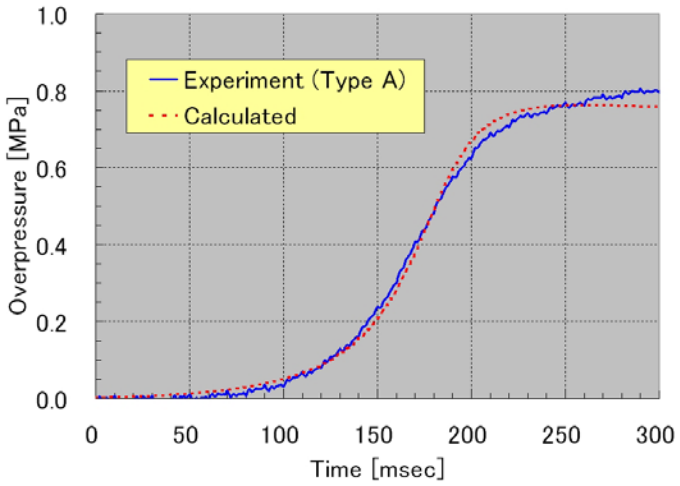

Fig. 10 Comparison of overpressure histories: experimental results and calculations

In the results calculated using the grids of the Type B chamber, obvious differences between the experimental and calculated values are presented by “maximum pressure” and “rise velocity." As considered in Fig. 5, maximum pressure drops when reaction heat is lost from the wall surface of the

chamber. In these calculations, the temperature of the wall surface is held at a constant value (namely, the existence of heat loss from the wall surface was neglected here); thus the main cause of not changing the maximum pressure shown in Fig.12 should be elucidated in conjunction with the constant temperature of the wall surface. On the other hand, the rise velocity is one of the elements that changes to a great extent depending on the values set for the FIRE calculation parameters. The rise velocity, in particular, is sensitive to changes in parameters determining initial flame surface immediately after ignition. The ignition system used in the explosion experiment conducted with the Type B chamber differs from that used in the explosion experiment with the present Type A chamber. Therefore, the ignition energies of both explosion experiments might be largely different from each other.

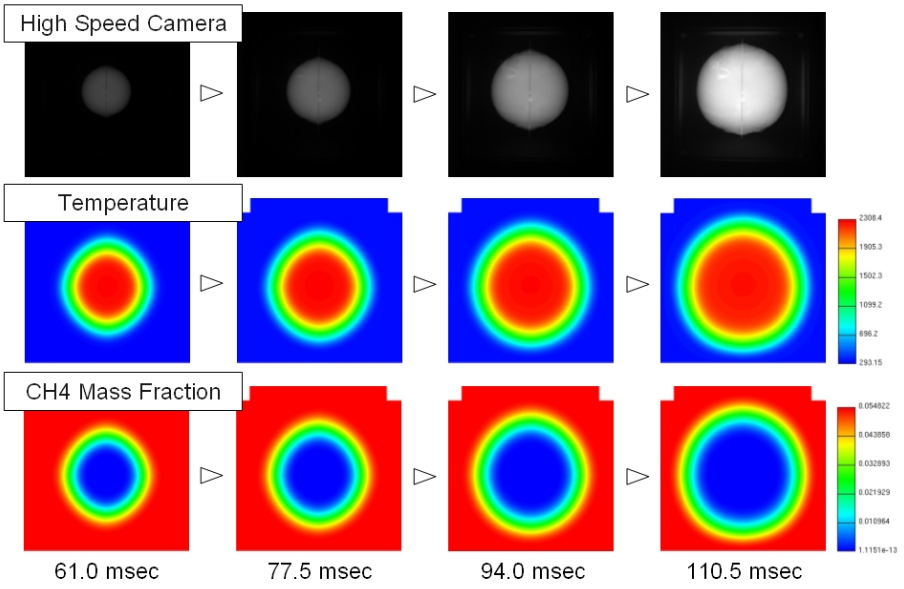

Fig. 11 Flame propagation (experiment vs. simulation)

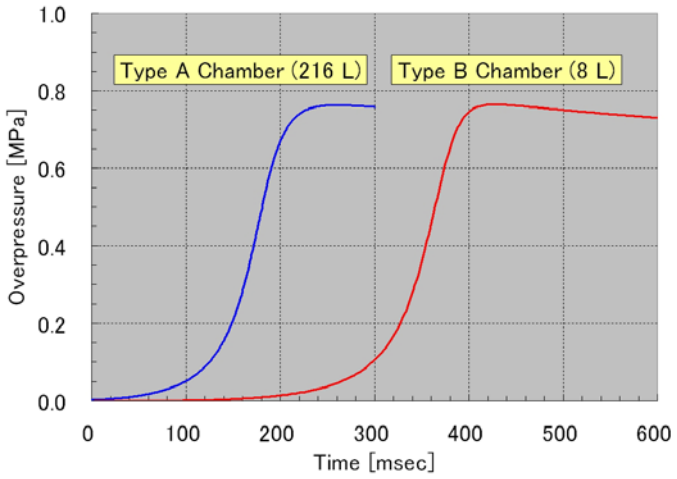

Fig.12 Comparison of overpressure histories in chambers of different volume using the same calculation parameters

5. Conclusion

Explosion experimentation was performed using a 0.21-m^3 constant-volume chamber. When comparing the results of an explosion experiment using a constant-volume chamber with an inner volume of 8 L conducted under the same conditions, a difference in the overpressure rise velocity, which was considered to be caused by a difference of spatial scale, was found. Based on the comparison, it is understood that discussions taking not only the conversion of the chamber size and time scale but also the detailed mechanism of the explosion phenomenon into consideration are indispensable in attempts to match overpressure rise velocities of two explosions with different scales.

In the explosion experiment provided with a vent area, a conspicuous difference regarding the occurrence of a 2nd pressure peak was found in addition to the aspects discussed above, but it is suggested this was caused by a difference of spatial scale as well as the difference in mass in the vent area. Until now, there have been extremely few examples that took the mass of the vent area into consideration in a pressure peak prediction formula[10]. It is considered that this knowledge is very significant for the analysis of gas explosion incidents.

In addition, the necessity of considering the scale dependence is also demonstrated by the calculations. As CFD software (FIRE) used in this study includes calculation parameters that directly affect flame propagation speed, pressure rise velocity, and maximum pressure, it is necessary to determine the appropriate values of the calculation parameters for each scale. Furthermore, in future studies, when creating the calculation grids for a constant-volume chamber having a vent area, modeling of the vent area might become problematic. When attempting reproduction calculation for an explosion experiment involving venting, normally, modeling takes place such that the vent area instantly disappears at a predetermined pressure (P_v). In other words, the mass of the vent area is neglected in the present model. A future issue will be determining how to model the mass effect of the vent area.

6. References (not revised yet)

1. Harris, R.J., The investigation and control of gas explosions in buildings and heating plant, E&FN Spon Ltd, New York, 1983.
2. D.P.J. McCann, G.O. Thomas, D.H. Edwards, Combustion and Flame, Volume 59, Issue 3, March 1985, Pages 233-250.
3. D.P.J. McCann, G.O. Thomas, D.H. Edwards, Combustion and Flame, Volume 60, Issue 1, April 1985, Pages 63-70.
4. J. Chao, C.R. Bauwens, S.B. Dorofeev, Proceedings of the Combustion Institute, Volume 33, 2011, Pages 2367-2374.
5. R.G. Zalosh, Journal of Loss Prevention in the Process Industries, Volume 13, 1979, Pages 98-110.
6. M.G. Cooper, M. Fairweather, J.P. Tite, Combustion and Flame, Volume 65, 1986, Pages 1-14.

7. Dal Jae Park, Anthony Ronald Green, Young Soon Lee, Young-Cheng Chen, Combustion and Flame, Volume 150, Issues 1-2, July 2007, Pages. 27-39.
8. Dal Jae Park, Young Soon Lee, Anthony Roland Green, Journal of Hazardous Materials, Volume 155, Issues 1-2, 30 June 2008, Pages 183-192.
9. Not published, the experiments were conducted by Tokyo Gas in 1980s'.
10. D.M. Solberg, J.A. Papas, E. Skramstad, Proceedings of Third International Symposium on Loss Prevention and Safety Promotion in the Process Industries, Volume 3, 1980, Pages 1295-1303.
11. V.V. Molkov, D. Makarov, J. Puttock, Journal of Loss Prevention in the Process Industries, Volume 19, Issues 2-3, March-May 2006, Pages 121-129.

7. List of Tables

8. List of Figures